

Distant RR Lyrae from HiTS: Exploring the Outskirts of the Milky Way

Gustavo Medina Toledo^{1,2}, Ricardo Muñoz¹, Kathy Vivas³,
Jeffrey Carlin⁴ and Francisco Förster^{2,5}

1. Departamento de Astronomía, Universidad de Chile, Casilla 36-D, Santiago, Chile.
2. Millenium Institute of Astrophysics MAS.
3. Cerro Tololo Inter-American Observatory, National Optical Astronomy Observatory, Casilla 603, La Serena, Chile.
4. LSST, 950 North Cherry Avenue, Tucson, AZ 85719, USA.
5. Center for Mathematical Modelling, Universidad de Chile, Av. Blanco Encalada 2120 Piso 7, Santiago, Chile.

This contribution presents the results from an RR Lyrae search using data from the High cadence Transient Survey (HiTS), which was carried out with the Dark Energy Camera (DECam) imager at the Blanco (4m) telescope on Cerro Tololo, Chile. HiTS is a campaign primarily aimed at detecting early supernovae explosions in real-time with the deep optical images DECam provides. However, the cadence and the strategy followed for the survey are well matched for RR Lyrae detection as well. Using data from the second and third year of the survey (2014A and 2015A), we were able to detect new RR Lyrae stars out to 200 kpc from the Sun, and to study their possible connection with known or previously undiscovered Milky Way satellite systems and halo substructures. Here we describe these tantalizing detections and further implications.

1 Introduction

Only a small number of remote Milky Way (MW) stars have been found at large heliocentric distances (d_H) in the halo of the Galaxy ($d_H > 100$ kpc). These stars are key probes of the accretion history of our Galaxy, since models suggest that they likely originated in relatively recently-accreted satellite galaxies (Bullock & Johnston, 2005). In fact, simulations suggest different behaviors of the inner and outer halo density profiles, where the inner halo is dominated by populations formed in-situ and the latter by the stellar component resulting from accretion events (Zolotov et al., 2009). In this sense, RR Lyrae variable stars (RRLs) have played an important role mapping the distant halo at large distances, since they are easily identified in time-series data and are intrinsically bright. However, only a few MW RRLs have been identified beyond 100 kpc to this day.

In addition, groups of RRLs at large distances have become important for the description of substructures in the outer halo. Because they are not expected to have formed in the outermost regions of the halo, the possible explanations for their positions seem to be limited. Since all known MW dwarf galaxies that have been searched for RRLs have at least one, some authors have proposed RRLs as potential tracers of faint satellite systems in the outer halo (Vivas et al., 2016). Here we report the detection of distant RRLs and associate them with these ideas.

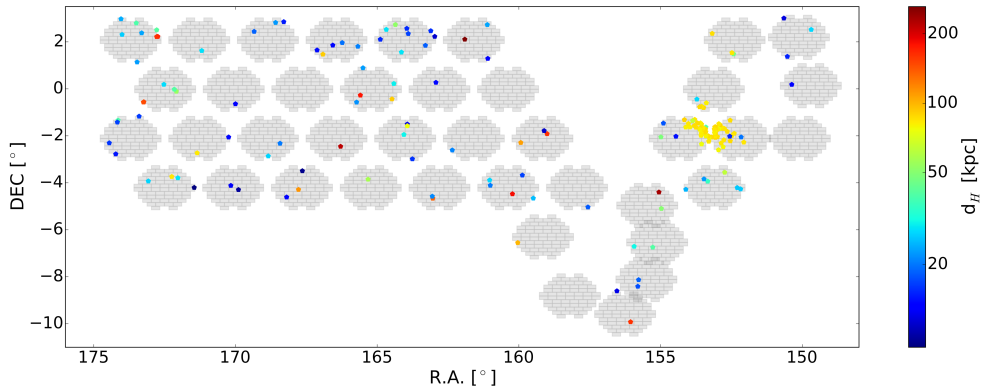


Fig. 1: Color-coded spatial distribution of the 173 RRLs from 2014. An approximation of the HiTS footprint is shown in grey in the background as a reference.

2 Observations and Methodology

We inspected data taken by the Dark Energy Camera (DECam) on the 4 m telescope at Cerro Tololo Interamerican Observatory, as part of the second and third campaign of the High cadence Transient Survey (HiTS). These campaigns were conducted during the semesters 2014A and 2015A. The survey is mainly focused on the detection and characterization of young supernovae events in real-time. The search strategy of HiTS makes use of images in the g -band (also r for 2015) for 40 (50) fields observed with a cadence of about two hours, during five (six) consecutive nights, with 160 s (87 s) exposures. Therefore, given that each DECam field covers about 3 sq. degrees of the sky, the total area covered by HiTS is 120 sq. degrees in 2014, and 150 sq. degrees in 2015. The survey's footprint in 2015 includes 14 fields already observed in the second campaign.

The extraction of the sources from the reduced images was performed using the photometry software **SExtractor** (Bertin & Arnouts, 1996). We performed relative photometry by calculating zero point values between all the epochs and a chosen reference epoch. Then, we calibrated our instrumental magnitudes with respect to the Pan-STARRS1 (PS1) 3π public catalogs (Sesar et al., 2017). For the extinction correction we used the recalibrated dust maps from Schlafly & Finkbeiner (2011). For the further analysis, we only considered objects with more than five detections and that show clear signs of variability. If r -band observations were available (2015), an additional cut was applied based on $g - r$ colors typical of RRLs. The period analysis was carried out by using the generalized Lomb-Scargle periodogram (GLS; Zechmeister & Kürster, 2009). Variables with periods shorter than 0.2 d and longer than 0.9 d were filtered out. We also filtered out stars with not statistically significant periods detected. Finally, a visual inspection of the phased light curves was applied to the stars with $\Delta\text{mag} > 0.2$, looking for periods, amplitudes, and light-curve shapes typical of RRLs. Our final lists of RRLs are comprised of 173 objects for 2014, and 159 for 2015. We used Sesar et al. (2017) PLZ relations to estimate values of absolute magnitudes M_g and subsequently heliocentric distances through

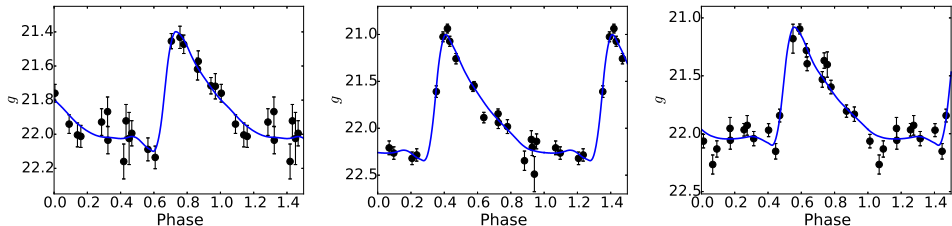


Fig. 2: Folded light curves for the three ab-type RRLs found in Leo V (HiTS113057+021331, HiTS113105+021319, and HiTS113107+021302, from left to right).

distance modulus, assuming $[\text{Fe}/\text{H}] = -1.5$ as the metallicity of the halo for most of the sample. The periods of the RRc subsample were first “fundamentalized” by using the transformation in Catelan (2009).

3 Results

The analysis of the data from the second HiTS campaign led to the detection of 173 RRLs, with mean g magnitudes ranging from ~ 15.5 to 22.8, and d_{H} between 9 and 260 kpc. Most of these RRLs are classified as R Rab (75%). In Figure 1, the spatial distribution of this sample is shown.

Figure 1 shows a clear overdensity of stars at $\text{RA} \simeq 153.3^\circ$, $\text{DEC} \simeq -1.7^\circ$ and $d_{\text{H}} \simeq 80$ kpc. The position of these stars matches the location of the Sextans dwarf spheroidal (dSph) galaxy. We found 65 RRLs located within 1.75 degrees of the dwarf galaxy, with d_{H} between 76 and 90 kpc (48 R Rab, 17 RRc). The HiTS fields do not cover the center of the Sextans dSph but only its outskirts. Given that previous surveys of RRLs in this galaxy have not covered its full extension, HiTS is providing for the first time information on the outermost RRLs in this dwarf galaxy. We report the discovery of 46 new RRLs in the Sextans dSph, which brings a total of 165 known RRLs in this galaxy. The distribution of the HiTS RRLs in the dwarf galaxy does not show evidence of substructures and all RRLs are contained within its known King limiting radius. We re-calculated the distances for the RRLs in the Sextans dSph adopting $[\text{Fe}/\text{H}] = -1.93 \pm 0.01$ from Kirby et al. (2011). Our final estimation of the mean d_{H} of the dSph is 84.2 ± 3.3 kpc, in agreement with previous studies. The mean period of the R Rab in the dwarf galaxy is 0.63 d, close to the nominal Oosterhoff II (Oo II) group, although the distribution the 65 RRLs does not follow a single sequence of Oosterhoff groups. This confirms the Oo-intermediate nature of this galaxy.

We also found two distant groups of RRLs that we associate with the Leo IV and Leo V ultra-faint dwarf (UFD) galaxies. We detected two of the three known RRLs in Leo IV (Moretti et al., 2009), consistent with our completeness estimations, and three RRLs in Leo V. Medina et al. (2017) detail the serendipitous discovery of these RRLs in Leo V, which was not explored for variability before. Figure 2 shows the light curves of these HiTS RRLs. The position of these stars in the color-magnitude diagram of the inner 5 arcmin of Leo V, as well as their spatial distribution are shown in the left/right panels of Figure 3. Medina et al. (2017) obtain corrected

distances for the Leo IV and Leo V RRLs by anchoring to the known distance of Leo IV (Moretti et al., 2009). An update of these distances is obtained by considering their metallicities. Assuming $[\text{Fe}/\text{H}] = -2.31$ for Leo IV (Simon & Geha, 2007) and $[\text{Fe}/\text{H}] = -2.48$ for Leo V (Collins et al., 2017), we get a mean d_{H} of 151.4 ± 4.4 kpc and 169.0 ± 4.4 kpc, respectively.

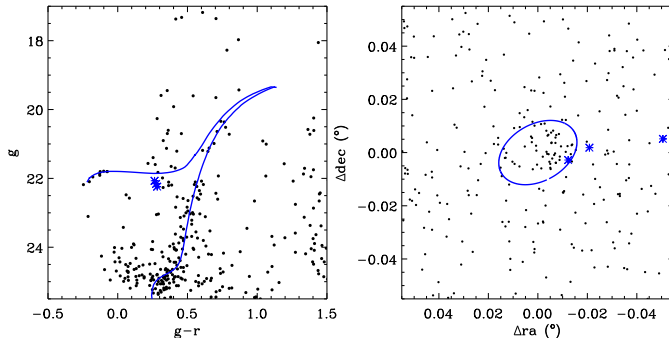


Fig. 3: Color-magnitude diagram of the inner 5 arcmin of Leo V (*left*) and their spatial distribution (*right*), using data from the Megacam survey (R. Muñoz et al, in preparation). Blue asterisks mark the position of our three RRLs in Leo V. Overplotted is a 13 Gyr old isochrone with $[\text{Fe}/\text{H}] = -2.2$ and $d_{\text{H}} = 175$ kpc (*left*), and a blue ellipse representing Leo V’s effective radius (*right*).

We find 18 RRLs within our list located at $d_{\text{H}} > 90$ kpc ($\langle g \rangle \geq 20.5$). Among this sample, 13 are found beyond the most distant previously known MW RRLs ($d_{\text{H}} > 130$ kpc). The distant RRLs span a range from 92 kpc to ~ 260 kpc. Medina et al. (2018) provide a detailed analysis of this sample. Regarding their classification, 61% of this faint subsample correspond to RRab, and three of the four most distant RRLs are *c*-type. In the Bailey diagram, these stars are mostly located close to the locus of the Oo II group, with a significantly different behavior compared with nearby HiTS RRLs. The mean period of the distant sample is similar to the one of RRLs in the UFD satellites of the MW. The latter might suggest that UFD galaxies are the main contributors of the outskirts of the halo.

With our sample of RRLs we studied the variation in the number of RRLs per unit volume, i.e., number density profiles. We used all 40 fields to build a profile as a single line of sight in the Galaxy, but excluding the RRLs in the Sextans dSph. We fitted a spherical (sph) and an ellipsoidal (ell) halo model to the data of the form $\rho(R) \sim R^n$, allowing a possible break to be detected. In the case of the ellipsoidal halo, we assumed an oblateness of $q = 0.7$. To find the posterior distributions for the parameters of the models we used the MCMC routine `emcee` (Foreman-Mackey et al., 2013). The best fit corresponds to the sph case, for which we obtain a simple power-law with $n = -4.17^{+0.18}_{-0.20}$. For a sph halo, if a broken power law is considered, the profile has a break at $R_b = 19.52^{+9.90}_{-3.27}$ kpc with an inner/outer slope of $n_1 = -3.50^{+1.98}_{-1.46}/n_2 = -4.22^{+0.32}_{-0.26}$.

A total of 159 RRLs constitute the preliminary list of RRLs in the HiTS 2015 data. These RRL candidates cover a range of 15.7 – 23.1 in g , and from -0.14 to 0.59 in $g - r$. As 14 of the fields of this campaign overlay fields from 2014, a

significant number of RRLs are present in both selections. Only 102 of the 159 RRLs are exclusive to the 2015 data, while the other 57 are mostly from the Sextans dSph. From the RRLs that are exclusive to HiTS 2015, 73 are RRab and 29 RRc types.

4 Final Remarks

We built a catalog with 332 RRLs using data from HiTS, with at least 18 of them located at $d_H > 90$ kpc. We analyzed the sample resulting from the search of RRLs in HiTS 2014, using it as an unprecedented probe of the outer halo. Additionally, we detected RRLs with a similar d_H distribution in the data from 2015. Baker & Willman (2015) suggested that groups of closely spaced RRLs in the halo (beyond 50 kpc) are good indications of the presence of satellites hard to detect by other methods. Our discovery of three distant RRLs matching the position of Leo V is a proof-of-concept of their idea. The behavior of the density profiles obtained are in agreement with accretion-only models (Bullock & Johnston, 2005), which supports the hypothesis of an outer halo made up completely of accreted stars. These results are part of a larger *LSST* precursor program we are conducting for mapping the limits of the outer halo, which will help the interpretation of the huge RRL samples *LSST* is expected to provide.

Acknowledgements. Powered@NLHPC: This research was partially supported by the supercomputing infrastructure of the NLHPC (ECM-02). This project used data obtained with the Dark Energy Camera (DECam), which was constructed by the Dark Energy Survey (DES) collaboration.

References

- Baker, M., Willman, B., *AJ* **150**, 160 (2015), [arXiv:1507.00734](#)
Bertin, E., Arnouts, S., *A&AS* **117**, 393 (1996)
Bullock, J. S., Johnston, K. V., *ApJ* **635**, 931 (2005), [arXiv:astro-ph/0506467](#)
Catelan, M., *Ap&SS* **320**, 261 (2009), [arXiv:astro-ph/0507464](#)
Collins, M. L. M., et al., *MNRAS* **467**, 573 (2017), [arXiv:1608.05710](#)
Foreman-Mackey, D., Hogg, D. W., Lang, D., Goodman, J., *PASP* **125**, 306 (2013), [arXiv:1202.3665](#)
Kirby, E. N., et al., *ApJ* **727**, 78 (2011), [arXiv:1011.4937](#)
Medina, G., et al., *ArXiv e-prints* (2018), [arXiv:1802.01581](#)
Medina, G. E., et al., *ApJ* **845**, L10 (2017), [arXiv:1708.00009](#)
Moretti, M. I., et al., *ApJ* **699**, L125 (2009), [arXiv:0906.0700](#)
Schlafly, E. F., Finkbeiner, D. P., *ApJ* **737**, 103 (2011), [arXiv:1012.4804](#)
Sesar, B., et al., *AJ* **153**, 204 (2017), [arXiv:1611.08596](#)
Simon, J. D., Geha, M., *ApJ* **670**, 313 (2007), [arXiv:0706.0516](#)
Vivas, A. K., et al., *AJ* **151**, 118 (2016), [arXiv:1510.05539](#)
Zechmeister, M., Kürster, M., *A&A* **496**, 577 (2009), [arXiv:0901.2573](#)
Zolotov, A., et al., *ApJ* **702**, 1058 (2009), [arXiv:0904.3333](#)